Quantitative Mass Spectrometry Analysis of Cerebrospinal Fluid Biomarker Proteins Reveals Stage-Specific Changes in Alzheimer's Disease

Caroline M. Watson[1], Eric B. Dammer[1], Lingyan Ping[1], Duc M. Duong[2], Erica Modeste[1], E. Kathleen Carter[2], Erik C. B. Johnson[1], Allan I. Levey[1*], James J. Lah[1*], Blaine R. Roberts[1,2], and Nicholas T. Seyfried[1,2*]

[1]Department of Neurology, [2]Department of Biochemistry, Emory University School of Medicine

* To whom correspondence should be addressed:

Nicholas T. Seyfried, PhD.
Departments of Biochemistry and Neurology
Rollins Research Building
1510 Clifton Road NE
Atlanta, GA 30322
Phone: 404-712-9783
Email: nseyfri@emory.edu

James J. Lah, MD, PhD.
Department of Neurology
Emory Brain Health Center
12 Executive Park Drive Northeast
Atlanta, GA 30329
Email: jlah@emory.edu

Allan I Levey, MD, PhD.
Department of Neurology
Goizueta Alzheimer's Disease Research Center
6 Executive Park Drive Northeast
Atlanta, GA 30329
Email: alevey@emory.edu

Abstract

Alzheimer's disease (AD) is the most common form of dementia, with cerebrospinal fluid (CSF) β-amyloid (Aβ), total Tau, and phosphorylated Tau providing the most sensitive and specific biomarkers for diagnosis. However, these diagnostic biomarkers do not reflect the complex changes in AD brain beyond plaque and tangle pathologies. Here we report a sensitive, quantitative, and scalable targeted proteomics assay of AD biomarkers representing mainly neuronal, glial, vasculature and metabolic pathways. As quality controls (QCs), we pooled CSF from individuals having normal Aβ and Tau levels (AT-), and individuals having low Aβ and high Tau levels (AT+) to determine the coefficient of variation (CV) and fold-change of protein measurements. Additionally, we analyzed 390 CSF samples using selective reaction monitoring-based mass spectrometry (SRM-MS). Following trypsin digestion, 133 controls (cognitively normal and AT-), 127 asymptomatic (cognitively normal and AT+) and 130 symptomatic AD (cognitively impaired and AT+), and 30 pooled CSF samples were analyzed by SRM-MS using a 15-minute targeted liquid chromatography-mass spectrometry method. Isotopically labeled peptide standards were added for relative quantification by reporting the area ratios for each targeted peptide. We reproducibly detected 62 peptides from 51 proteins in all clinical samples with an average CV of approximately 13% across pools. Proteins that could best distinguish AsymAD and AD cases from controls included SMOC1, GDA, 14-3-3 proteins, and proteins involved in glucose metabolism. In contrast, proteins that could best distinguish AD from AsymAD were mainly neuronal/synaptic proteins including VGF, NPTX2, NPTXR, and SCG2. Collectively, this highlights the utility of high-throughput SRM-MS to quantify peptide biomarkers in CSF that can potentially monitor disease progression.

Background and Summary

Alzheimer's disease (AD) affects more than 45 million people worldwide, making it the most common neurodegenerative disease [1-3]. AD biomarker research has predominately focused on β-amyloid (Aβ) and Tau, as these proteins reflect pathological Aβ plaques and tau neurofibrillary tangles (NFT), respectively, in AD [4, 5]. Although Aβ and Tau are the most sensitive and specific CSF biomarkers for diagnosis [6, 7] these two proteins do not reflect the heterogenous and complex changes in AD brain [8, 9]. Furthermore, failed clinical trials of Aβ-based therapeutic approaches highlight the complexity of AD and the need for additional biomarkers to fully illustrate pathophysiology for advancements in diagnostic profiling, disease monitoring, and treatments [1-3, 9].

Considering the diagnostic challenges related to the overlapping pathologies of neurodegenerative diseases, AD biomarkers that represent diverse pathophysiological changes could facilitate an early diagnosis, predict disease progression, and enhance the understanding of neuropathological changes in AD [3]. AD has a characteristic pre-clinical or asymptomatic period (AsymAD) where individuals have AD neuropathology in the absence of clinical cognitive decline [5, 10, 11]. Thus, biomarkers for the prodromal phase of AD that can begin changing years or decades before signs of cognitive impairment, would be valuable for disease intervention, clinical trial stratification, and monitoring drug efficacy.

Proteins are the proximate mediators of disease, integrating the effects of genetic, epigenetic, and environmental factors [9, 12]. Network proteomic analysis has emerged as a valuable tool for organizing complex unbiased proteomic data into groups or "modules" of co-expressed proteins that reflect various biological functions [13-16]. The direct proximity of CSF to the brain presents a strong rationale to integrate the brain and CSF proteomes to increase the pathophysiological diversity among biofluid biomarkers of AD [7, 17]. We recently integrated a human AD brain proteomic network with a CSF proteome differential expression analysis to reveal approximately 70% of the CSF proteome overlapped with the brain proteome [18]. Nearly 300 CSF proteins were identified as significantly altered between control and AD samples, representing predominately neuronal, glial, vasculature and metabolic pathways, creating an excellent list of candidates for further quantification and validation.

Here, we developed a high-throughput targeted selective reaction monitoring-based mass spectrometry (SRM-MS) assay [19] to quantify and validate reliably detected CSF proteins in healthy individuals and individuals with asymptomatic or symptomatic AD for staging AD

progression. We evaluated 200+ tryptic peptides that were selected using a data-driven approach from the integrated brain-CSF proteome network analysis. We selected peptides with differential abundance in AD CSF observed >50 percent of case samples by discovery proteomics [18] for synthesis as crude heavy standards. We used two pooled CSF reference standards to determine which peptides were reliably detected in CSF matrix. We reproducibly detected 62 tryptic peptides from 51 proteins in 390 clinical samples and 30 pooled reference standards. Furthermore, using a combination of differential expression and receiver operating curve (ROC) analyses we found CSF proteins that can best discriminate stages of AD progression. Collectively these data highlight the utility of a high throughput SRM-MS approach to quantify biomarkers associated with AD that ultimately hold promise for monitoring disease progression, stratifying patients for clinical trials, and measuring therapeutic response.

Methods

Reagents and Materials

Heavy labeled PEPotec Grade 2 crude peptides, trypsin, mass spectrometry grade, trifluoroacetic acid (TFA), foil heat seals (AB-0757), and low-profile square storage plates (AB-1127) were purchased from ThermoFisher Scientific (Waltham, MA). Lysyl endopeptidase (Lys-C), mass spectrometry grade was bought from Wako (Japan); sodium deoxycholate, CAA (chloroacetamide), TCEP (tris-2(-carboxyethyl)-phosphine), and triethylammonium hydrogen carbonate buffer (TEAB) (1 M, pH 8.5) were obtained from Sigma (St. Louis, MO). Formic acid (FA), 0.1% FA in acetonitrile, 0.1% FA in water, methanol, and sample preparation V-bottom plates (Greiner Bio-One 96-well Polypropylene Microplates; 651261) are from Fisher Scientific (Pittsburgh, PA). Oasis PRiME HLB 96-well, 30mg sorbent per well, solid phase extraction (SPE) cleanup plates were from Waters Corporation (Milford, MA).

Pooled CSF as Quality Controls

Two pools of CSF were generated based on Aβ(1-42), total Tau, and pTau181 levels to create AD-positive (AT+) and AD-negative (AT-) quality control standards. Each pool consisted of approximately 50 mL of CSF by combining equal volumes of CSF selected from well characterized samples (~45 unique individuals per pool) from the Emory Goizueta Alzheimer's Disease Research Center (ADRC) and Emory Healthy Brain Study (EHBS). All research participants provided informed consent under protocols approved by the Institutional Review Board (IRB) at Emory University. CSF was collected by lumbar puncture and banked according to 2014 ADC/NIA best practices guidelines (https://www.alz.washington.edu/BiospecimenTaskForce.html). AD biomarker status for individual cases was determined on the Roche Elecsys® immunoassay platform [20-22]; the average CSF biomarker value is reported in parentheses. The control CSF pool (AT-) was comprised of cases with relatively high levels of Aβ(1-42) (1457.3 pg/mL) and low total Tau (172.0 pg/mL) and pTau181 (15.1 pg/mL). In contrast, the AD pool (AT+) was comprised of cases with low levels of Aβ(1-42) (482.6 pg/mL) and high total Tau (341.3 pg/mL) and pTau181 (33.1 pg/mL). The quality control (QC) pools were processed and analyzed identically to the CSF clinical samples reported.

Clinical Characteristics of the Cohort

Human cerebrospinal fluid (CSF) samples from 390 individuals including 133 healthy controls, 130 patients with symptomatic AD, and 127 patients asymptomatic AD (cognitively normal but AD

biomarker positive) were obtained from Emory's Goizueta ADRC and EHBS (**Figure 1 and Table 1**). All symptomatic individuals were diagnosed by expert clinicians in the ADRC and Emory Cognitive Neurology Program, who are subspecialty trained in Cognitive and Behavioral Neurology, following extensive clinical evaluations including detailed cognitive testing, neuroimaging, and laboratory studies. CSF samples were selected to balance for age and sex (**Table 1**). For biomarker measurements, CSF samples from all individuals were assayed for Aβ(1-42), total Tau, and pTau using the Roche Diagnostics Elecsys® immunoassay platform [20-22]. The cohort characteristics are summarized in **Figure 1 and Table 1**. Samples were stratified into controls, AsymAD and AD based on Tau and Amyloid biomarkers status and cognitive score (MoCA). All case metadata (syn34612929) including disease state, age, sex, race, apolipoprotein (ApoE) genotype, MoCA scores, and biomarkers measurements were deposited on Synapse (syn34054965) [Data citation 1].

Single Reaction Monitoring Assay

We selected 200+ peptides with differential abundance in AD CSF by discovery proteomics [18, 23] for synthesis as crude heavy standards. The heavy crude peptides contained isotopically labeled C-terminal lysine or arginine residues (^{13}C, ^{15}N) for each tryptic peptide. Based on the crude heavy peptide signal, the peptides were pooled to achieve total area signals ≥ $1x10^5$ in CSF matrix. The transition lists were created in Skyline-daily software (version 21.2.1.455) [24, 25]. An in-house spectral library was created in Skyline based on tandem mass spectra from CSF samples. Skyline parameters were specified as: trypsin enzyme, Swiss-Prot background proteome, and carbamidomethylation of cysteine residues (+57.02146 Da) as fixed modifications. Isotope modifications included: 13C(6)15N(4) (C-term R) and 13C(6)15N(2) (C-term K). The top ten fragment ions that matched the criteria (precursor charges: 2; ion charges 1, 2; ion types: y, b; product ion selection from m/z >precursor to last ion-2) were selected for scrutiny. The top 5-7 transitions per heavy precursor were selected by manual inspection of the data in Skyline and scheduled transition lists were created for collision energy optimization. Collision energies were optimized for each transition; the collision energy was ramped around the predicted value in 3 steps on both sides, in 2V increments [26]. The selected transitions were tested in real matrix spiked with the heavy peptide mixtures. The three best transitions per precursor were selected by manual inspection of the data in Skyline and one scheduled transition list was created for the final assays. A list of transitions (syn34615929) used in this study is deposited on Synapse (syn34054965) [Data citation 2].

Preparation of CSF for mass spectrometric analysis

All CSF samples were blinded and randomized. Each CSF sample was thawed and aliquoted into sample preparation V-bottom plates that also included quality controls. Each sample and quality control were processed independently in parallel. Crude CSF (50 µL) was reduced, alkylated, and denatured with tris-2(-carboxyethyl)-phosphine (5 mM), chloroacetamide (40 mM), and sodium deoxycholate (1%) in triethylammonium bicarbonate buffer (100 mM) in a final volume of 150 µL. Sample plates were heated at 95°C for 10 min, followed by a 10-min cool down at room temperature while shaking on an orbital shaker (300 rpm) [27]. CSF proteins were digested with Lys-C (Wako; 0.5 µg; 1:100 enzyme to CSF volume) and trypsin (Pierce; 5 µg; 1:10 enzyme to CSF volume) overnight in a 37°C oven. After digestion, heavy labeled standards for relative quantification (15 µL per 50 µL CSF) were added to the peptide solutions followed by acidification to a final concentration of 0.1% TFA and 1% FA (pH ≤ 2). Sample plates were placed on an orbital shaker (300 rpm) for at least 10 minutes to ensure proper mixing. Plates were centrifuged (4680 rpm) for 30 minutes to pellet the precipitated surfactant. Peptides were desalted with Oasis PRiME HLB 96-well, 30mg sorbent per well, solid phase extraction (SPE) cleanup plates from Waters Corporation (Milford, MA) using a positive pressure system. Each SPE well was conditioned (500 µL methanol) and equilibrated twice (500 µL 0.1% TFA) before 500 µL 0.1% TFA and supernatant were added. Each well was washed twice (500 µL 0.1% TFA) and eluted twice (100 µL 50% acetonitrile/0.1% formic acid). All eluates were dried under centrifugal vacuum and reconstituted in 50 µL mobile phase A (0.1% FA in water) containing Promega 6 × 5 LC-MS/MS Peptide Reference Mix (50 fmol/µL; Promega V7491).

Liquid chromatography-tandem mass spectrometry (LC-MS/MS)

Peptides were analyzed using a TSQ Altis Triple Quadrupole mass spectrometer (Thermo Fisher Scientific). Each sample was injected (20 µL) using a 1290 Infinity II system (Agilent) and separated on an AdvanceBio Peptide Map Guard column (2.1x5mm, 2.7 µm, Agilent) connected to AdvanceBio Peptide Mapping analytical column (2.1x150mm, 2.7 µm, Agilent). Sample elution was performed over a 14-min gradient using mobile phase A (MPA; 0.1% FA in water) and mobile phase B (MPB; 0.1% FA in acetonitrile) with flow rate at 0.4 mL/min. The gradient was from 2% to 24% MPB over 12.1 minutes, then from 24% to 80% over 0.2 min and held at 80% B for 0.7 min. The mass spectrometer was set to acquire data in positive-ion mode using single reaction

monitoring (SRM) acquisition. Positive ion spray voltage was set to 3500 V for the Heated ESI source. The ion transfer tube and vaporizer temperatures were set to 325°C and 375°C, respectively. SRM transitions were acquired at Q1 resolution 0.7 FWHM, Q2 resolution 1.2 FWHM, CID gas 1.5 mTorr, 0.8 s cycle time.

Data analysis

Raw files from Altis TSQ were uploaded to Skyline-daily software (version 21.2.1.455), which was used for peak integration and quantification by peptide ratios. SRM data were manually evaluated. All samples were analyzed in a blinded fashion. Total area ratios for each peptide were calculated in Skyline by summing the area for each light (3) and heavy (3) transition and dividing the light total area by the heavy total area. We used the total area ratios (peptide ratios) for each targeted peptide in each sample and QC analysis. The raw data files (syn34054983) and Skyline file (syn34055004) were deposited on Synapse (syn34054965) [Data citation 3].

Statistical analyses

We used Skyline-daily software (version 21.2.1.455) and GraphPad Prism (version 9.4.1) software to calculate means, medians, standard deviations, and coefficients of variations [25]. Peptide abundance ratios were log2-transformed, and zero values were imputed as one-half the minimum nonzero abundance measurement. Then, one-way ANOVA with Tukey *post hoc* tests for significance of the paired groupwise differences across diagnosis groups was performed in R using a custom calculation and volcano plotting framework implemented and available as an open-source set of R functions documented further on https://www.github.com/edammer/parANOVA. T test p values and Benjamini-Hochberg FDR for these are reported for two total group comparisons, as was the case for AT+ versus AT- peptide mean difference significance calculations. Receiver-operating characteristic (ROC) analysis was performed in R version 4.0.2 with a generalized linear model binomial fit of each set of peptide ratio measurements to the binary case diagnosis subsets AD/Control, AsymAD/Control, and AD/AsymAD using the pROC package implementing ROC curve plots, and calculations of AUC and AUC DeLong 95% confidence interval. Additional ROC curve characteristics including sensitivity, specificity, and accuracy were calculated with the reportROC R package. Venn diagrams were generated using the R vennEuler package, and the heatmap was produced using the R pheatmap package/function. R boxplot function output was overlaid with beeswarm-positioned individual measurement points using the R beeswarm package. Pearson correlations of SRM peptide measurements to immunoassay measurements of Aβ(1-42), total Tau, phosphor-

T181 Tau, and the ratio of total Tau/ Aβ were performed using the corAndPvalue WGCNA function in R. Correlation scatterplots were generated using the verboseScatterplot WGCNA function.

Data Records

All files have been deposited on Synapse (syn34054965). These include sample traits (syn34612929, Data Citation 1), transition details (syn34615929, Data Citation 2), all mass spectrometry raw files (N=423) from both quality control replicates and clinical samples (syn34054983, Data Citation 3), Skyline quantification file (syn34055004, Data Citation 4), the peptide ratio data matrix (syn34615930, Data Citation 5), protein details (syn34615931, Data Citation 6), and QC statistics (syn34615928, Data Citation 7), and the ANOVA analysis results (syn34635281, Data Citation 8).

Technical Validation

Assessing peptide precision using pooled CSF quality control (QC) standards

We generated two pools of CSF reference standards as QCs based on biomarker status (AT- and AT+). These QCs were processed and analyzed (at the beginning, end, and after every 20 samples per plate) identically to the individual clinical samples for testing assay reproducibility. We analyzed 30 QCs (15 AT- and 15 AT+) over approximately 5 days during the run of clinical samples. We identified 62 peptides from 51 proteins as reliably measured in the pooled reference standards. We included 58 peptides from 51 proteins in our biomarker analysis, plus peptides specific for the four APOE alleles for proteogenomic confirmation of APOE genotypes [28, 29]. The technical coefficient of variation (CV) of each peptide was calculated based on the peptide area ratio for the biomarker negative (AT-) and positive (AT+) QCs. We defined CSF peptide biomarkers with CVs ≤ 20% as quantified with high precision in these technical replicates which were un-depleted and unfractionated CSF sample pools. Technical and process reproducibility for all reported peptides was below 20% (CV < 20%) in at least one pooled reference standard (**Supplemental Figure 1**). **Supplemental Table 1** contains the QC statistics for the biomarker and APOE allele specific peptides. Levels of HBA and HBB peptides can be used to assess the levels of potential blood contamination [30] in each of the CSF samples across individual plates (**Supplemental Figure 2**). Correction for blood contamination could improve the statistics; however, no correction was performed for the statistical analyses presented. We used the protein

directions of change to assess accuracy in the QC pools. The volcano plot between peptides measured in the pools highlights peptide/protein levels that are consistent with previously reported AD biomarkers **(Supplemental Figure 3)** [18, 23].

Monitoring LC-MS/MS Instrument Performance

The sample reconstitution solution contained Promega 6×5 LC-MS/MS Peptide Reference Mix (50 fmol/µL) [31]. The Promega Peptide Reference Mix provides a convenient way to assess LC column performance and MS instrument parameters, including sensitivity and dynamic range. The mix consists of 30 peptides; 6 sets of 5 isotopologues of the same peptide sequence, differing only in the number of stable, heavy-labeled amino acids incorporated into the sequence using uniform ^{13}C and ^{15}N atoms making them chromatographically indistinguishable. The isotopologues were specifically synthesized to cover a wide range of hydrophobicities so that dynamic range could be assess across the gradient profile (**Figure 2A**). Each isotopologue represents a series of 10-fold dilutions, estimated to be 1 pmole, 100 fmole, 10 fmole, 1 fmole, and 100 amole for each peptide sequence in a 20 µL injection, a range that would challenge the lowest limits of detection of the method (**Figure 2B**). We assessed the raw peak areas in 423 injections over 5 days to determine the label-free CV for each peptide isotopologue (**Figure 2B**). The 100 amole level (0.0001x) was not detected (ND) for any of the peptide sequences. Based on the label-free CV, we determined the lowest limit of detection for each peptide to be between 1-10 fmole across the gradient profile with a dynamic range spanning 4 orders of magnitude for all peptides except the latest eluting peptide at 13.3 minutes (**Figure 2C**).

Technical Replicate Variance

Three individual samples were analyzed in duplicate scattered throughout the sample run sequence to assess technical replicate variance. We graphed the $\log_2$(ratio) for each of 58 biomarker peptides in replicate 1 versus replicate 2 for each sample and determined the Pearson correlation coefficient with associated P value (**Figure 3**). The analysis showed a near-identical correlation (ρ=0.996-0.998) between each of the technical replicate pairs for the three individual CSF samples, supporting the same high level of method reproducibility we found using the QC pools.

Usage Notes

Ultimately, this targeted mass spectrometry dataset serves as a valuable resource for a variety of research endeavors including, but not limited to, the following applications:

Use case 1: Peptide abundance in CSF

This dataset provides a reference for peptide detectability in CSF under relatively high-throughput conditions, especially if an investigator wants to determine whether their protein of interest has abundance above the lower limit of detection in CSF under these analytical conditions. Raw data contains transitions for over 200 peptides that were robustly detected in CSF discovery proteomics [18, 23]. [Data Citation 3].

Use case 2: Using APOE allele specific peptides for genotyping

Apolipoprotein E (ApoE) has three major genetic variants (E2, E3, and E4, encoded by the ε2, ε3 and ε4 alleles, respectively) that differ by single amino acid substitutions [32]. APOE genotype is closely related to AD risk [33] with ApoE4 having the highest risk, ApoE2 the lowest risk, and ApoE3 with intermediate risk [34, 35]. Due to the amino acid substitutions in each variant, there are allele specific peptides that can be targeted by mass spectrometry [28, 36]. We monitored CLAVYQAGAR (APOE2), LGADMEDVR (APOE4), LGADMEDVCGR (APOE2 or APOE3), and LAVYQAGAR (APOE3 or APOE4) to determine the APOE genotype of each CSF sample in a concurrent SRM-MS method [Data citation 1]. The CV for each APOE peptide in each QC is listed in **Supplemental Table 1**. Previous studies report the association of APOE genotype with various clinical, neuroimaging, and biomarker measures [37-40]. Exploring the relationship between APOE status and the CSF biomarker peptides presented requires further analysis reserved for future studies.

Use case 3: Stage-specific differences in peptide and protein levels

The described cohort includes control, AsymAD and AD groups across the Amyloid/Tau/Neurodegeneration (AT/N) framework [41], which allows for the comparison of peptide and protein differential abundance across stages of disease. Investigators can focus on comparisons that are specific to symptomatic AD or those with potential for staging AD by using the AsymAD group compared to the control group. By comparing candidate biomarkers using

ANOVA (excluding APOE allele specific peptides), we found 41 differentially expressed peptides (36 proteins) in AsymAD vs controls (**Figure 4A**), 35 differentially expressed peptides (30 proteins) in AD versus controls (**Figure 4B**), and 21 differentially expressed peptides (18 proteins) in AD vs AsymAD (**Figure 4C**). The Venn diagram summarizes the differentially expressed peptides across groups in **Figure 4D**.

Use case 4: Stratifying early from progressive biomarkers of AD

Using a differential abundance analysis, we were able to stratify the changing proteins as early or progressive biomarkers of AD (**Figures 4 and 5**). The $\log_2$-fold change (Log_2 FC) from the volcano plots in **Figure 4** are represented as a heatmap in **Figure 5A** to illustrate how each peptide is changing across each group comparison. Twenty-two peptides (21 proteins) were early biomarkers of AD because they were significantly different in AsymAD versus controls, but not significantly different in AD versus AsymAD (**Figure 5A**). A plurality of these proteins mapped to metabolic enzymes linked to glucose metabolism (PKM, MDH1, ENO1, ALDOA, ENO2, LDHB, and TPI1, also in **Supplemental Table 2**) [15, 16]. SMOC1 and SPP1, markers linked to glial biology and inflammation [16, 18], were also increased in AsymAD samples compared to controls (**Figure 5B**, *top row*). GAPDH, YWHAB and YWHAZ proteins were found to be progressive biomarkers of AD because the proteins were differentially expressed from Control to AsymAD and from AsymAD to AD with a consistent trend in direction of change (**Figure 5B**, *middle row*). Proteins associated with neuronal/synaptic markers including VGF, NPTX2, NPTXR, and L1CAM were increased in AsymAD compared to controls but decreased in AD vs controls (**Figure 5B**, *lower row*). Interestingly, we found 14 peptides (13 proteins) that were up in AsymAD as compared to Control but down in AD when compared to AsymAD. A majority of these proteins map to neuronal/synaptic markers including VGF, NPTX2, NPTXR, which are some of the most correlated proteins in post-mortem brain to an individual's slope of cognitive trajectory in life (**Figure 5A and 5B,** *lower row*) [42].

Use case 5: Correlation of peptide biomarker abundance to Aβ(1-42), Tau, pTau and cognitive measures

The comparison of existing biomarkers to the SRM peptide measurements can be accomplished by correlation, where the degree of correlation indicates how similar a peptide measurement is to the established immunoassay-measured biomarkers of Aβ(1-42), total Tau, and pTau as well as cognition (MoCA score). In **Figure 6A**, we demonstrate that 57 of the 58

biomarker peptides have significant correlation to at least one of the above biomarkers, or the ratio of total Tau/Aβ. Individual correlation scatterplots and linear fit lines for three of the peptides (SMOC1: AQALEQAK, YWHAZ: VVSSIEQK, and VGF: EPVAGDAVPGPK) are provided in **Figure 6B**. Significant correlations of these peptides to the established biomarker and cognitive measures indicate the potential of these measurements to classify or stage disease progression. The targeted SRM measurement correlations largely agree with those observed from unbiased discovery proteomics [43] and parallel reaction monitoring [23] experiments.

Use case 6: Receiver-operating characteristic (ROC) analysis for evaluating biomarker diagnostic capability

The capacity for peptide measurements to serve as a diagnostic biomarker distinguishing individuals with AD and even asymptomatic disease from individuals not on a trajectory to develop AD is well-established, with secreted amyloid and tau peptide measurements in CSF being the current gold standard for interrogation of patients' AD stage from their CSF [44] where CSF Aβ(1-42) concentration inversely correlates to plaque deposition in the living brain [45]. The measurements of additional peptides collected here are appropriate for comparison to immunoassay measurements of CSF amyloid and Tau biomarker positivity, or a dichotomized cognition rating, or other ancillary traits such as diagnosis for the 390 individuals can be performed. To demonstrate this utility, we performed receiver-operating characteristic (ROC) curve analysis and calculated the area under the curve (AUC) for all 62 peptide measures as fitting a logistic regression to 3 subsets of samples divided to represent known pairs of disease stages, namely AD versus control, AsymAD versus control, and AD vs AsymAD (**Figure 7** and **Supplemental Table 4**). The top performing peptide for the YWHAZ gene product 14-3-3 ζ protein demonstrated an AUC of 90% discrimination of AD from control cases consistent with previous studies [23, 46, 47]. SMOC1 AUC of 81.8% was the best performing peptide for discrimination of AsymAD from control groups. Given the enrichment of APOE4 carriers in the AsymAD group, the APOE4 allele specific peptide LGADMEDVR was also an excellent classifier (AUC 78.4%) of AsymAD versus control groups. In contrast, the synaptic peptides to NPTX2 (AUC of 74.0%), NPTXR (AUC of 71.1%), VGF (AUC of 70.1%) and SCG2 (AUC of 69.8%) best discriminated AD from AsymAD groups suggesting that neurodegeneration due to AD pathology is occurring in the symptomatic phase of disease [48]. **Figure 7** shows the top five peptides by AUC for each of the three comparisons, highlighting the potential of this data set to aid in the design or validation of stage-specific biomarkers. Additional future analysis using these peptides alone or in combination could be used to subtype, predict disease onset, and gauge treatment efficacy.

Use case 7: Absolute quantification of AD peptide/protein biomarkers

Typically, relative quantification is a precursor to nominating biomarkers for absolute quantification using purified synthetic standards. The peptide-specific characteristics, such as intensity, charge state, and modification state, may serve as a resource to reference for future studies to determine the molar amount of AD biomarker peptides in CSF. Absolute quantification is an important step to defining cutoffs that could be used in a diagnostic or cohort classification.

Data Citations

1. Watson CM, Dammer EB, and NT. SAGE BIONETWORKS. Synapse ID: syn34054965.
2. Watson CM, Dammer EB, and Seyfried NT. SAGE BIONETWORKS. Synapse ID: syn34615929.
3. Watson CM, Dammer EB, and Seyfried NT. SAGE BIONETWORKS. Synapse ID: syn34054983.
4. Watson CM, Dammer EB, and Seyfried NT. SAGE BIONETWORKS. Synapse ID: syn34055004.
5. Watson CM, Dammer EB, and Seyfried NT. SAGE BIONETWORKS. Synapse ID: syn34615930.
6. Watson CM, Dammer EB, and Seyfried NT. SAGE BIONETWORKS. Synapse ID: syn34615931
7. Watson CM, Dammer EB, and Seyfried NT. SAGE BIONETWORKS. Synapse ID: syn34615928.

Acknowledgements

This study was supported by the following National Institutes of Health funding mechanisms: U01AG061357 (A.I.L and N.T.S), R01AG070937-01 (J.J.L) and P30AG066511 (A.I.L). We acknowledge our colleagues at Emory for providing critical feedback.

Disclosures

A.I.L, N.T.S. and D.M.D. are co-founders of Emtherapro Inc.

Data Availability

Raw mass spectrometry and pre- and post- processed peptide abundance data can be found at https://www.synapse.org/#!Synapse:syn34054965. The results published here are in whole or in part based on data obtained from the AMP-AD Knowledge Portal

(https://adknowledgeportal.synapse.org) by the AMP-AD Target Discovery Program and other programs supported by the National Institute on Aging to enable open-science practices and accelerate translational learning. The data, analyses, and tools are shared early in the research cycle without a publication embargo on secondary use. Data are available for general research use according to the following requirements for data access and data attribution (https://adknowledgeportal.synapse.org/#/DataAccess/Instructions).

Figure Legends

Figure 1. Cohort Characteristics. A total of 390 samples (133 controls, 127 AsymAD, 130 AD unless otherwise noted) were analyzed using the following characteristics for grouping. (**A**) Age range across each group of the cohort was carefully selected to balance for age and sex (**Supplemental Table 1**). (**B**) Cognition was assessed using the Montreal Cognitive Assessment (MoCA) score; there is no significant difference in scores between the Control and AsymAD groups serving as the two cognitively normal diagnostic groups (133 controls, 127 AsymAD, 124 AD). The Roche Diagnostics Elecsys® platform was used for CSF biomarker measurements for Aβ(1-42) (**C**), Total Tau (133 controls, 127 AsymAD, 129 AD) (**D**), and pTau (**E**) (pg/mL) showing the significance between groups for each measurement. (**F**) Tau/Aβ ratio data across control, AsymAD and AD groups. There was no significant difference between AsymAD and AD groups to serve as our biomarker positive groups (133 controls, 127 AsymAD, 129 AD). The significance of the pairwise comparisons is indicated by overlain annotation of 'ns' (not significant; $p>0.05$) or asterisks; ****$p\leq0.0001$.

Figure 2. Isotopologue peptide internal reference standards to determine consistency of LC-MS/MS platform. Each of the CSF samples were spiked with a six-peptide, 5 isotopologue concentration LC-MS/MS Peptide Reference Mix from Promega (50 fmol/µL). (**A**) Extracted ion chromatogram for the 6 peptide (1pmol) mixture illustrating the wide range of retention times due to their hydrophobicity. (**B**) The raw peak areas in 423 injections over 5 days were used to determine the label-free CV for each peptide isotopologue estimating the lowest limits of detection to be between 1-10 fmole for each peptide. (**C**) The 5 unique isotopologues are used to assess the dynamic range across the gradient profile and each peptide demonstrates linearity across 3-4 orders of magnitude in the batch of 423 injections. Error bars represent the standard deviation across 423 injections.

Figure 3. Technical reproducibility of peptide measurements in replicate CSF samples. Pearson correlation and p-value of replicate measures of 58 peptides in the 3 replicated CSF samples that were analyzed randomly within the series of 423 injections by SRM-MS.

Figure 4. Differential expression analysis across stages of AD. ANOVA analysis with Tukey *post hoc* FDR was performed for pairwise comparison of mean $\log_2$(ratio) differences between the 3 stages of AD (i.e., Control, AsymAD and AD) of N=390 total case samples and plotted as a volcano. Significance threshold for counting of peptides was ($p < 0.05$; dashed horizontal line).

Differentially expressed peptides for (**A**) AsymAD (N=127) versus control (N=133), (**B**) AD (N=130) versus control, and (**C**) AD versus AsymAD are labeled by their gene symbols. (**D**) Counts of peptides with significant difference in any of the 3 dichotomous comparisons are presented as a Venn diagram. Full statistics from the ANOVA and Tukey post-hoc analysis is presented in **Supplemental Table 2**.

Figure 5. Stratifying early from progressive biomarkers of AD. (**A**) The magnitude of positive (red) and negative (blue) changes are shown on a gradient color scale heatmap representing mean log_2-fold change (Log_2FC) for each of 49 peptides significant in any of the 3 group comparisons. Tukey significance of the pairwise comparisons is indicated by overlain asterisks; *p<0.05, **p<0.01, ***p<0.001. (**B**) Peptide abundance levels of selected panel markers that are differentially expressed between groups. The upper row highlights biomarkers that are significantly different in AsymAD versus controls, but not significantly different in AsymAD versus AD. The middle row of 3 peptides highlights progressive biomarkers of AD, which show a stepwise increase in abundance from control to AsymAD to AD cases. The bottom row highlights a set of proteins that are increased in AsymAD compared to controls but decreased in AD versus control or AsymAD samples.

Figure 6. Correlating CSF peptide biomarker abundances to amyloid, Tau, and cognitive measures. (**A**) Positive (red) and negative (blue) Pearson correlations between biomarker peptide abundance and immunoassay measures of Aβ(1-42), total Tau, phospho-T181 Tau (pTau), ratio of total Tau/Aβ and cognition (MoCA score). Student's significance is indicated by overlain asterisks; *p<0.05, **p<0.01, ***p<0.001. (**B**) Individual correlation scatterplots are shown for SMOC1 (upper row), YWHAZ (middle row), and VGF (lower row). Individual cases are colored by their diagnosis; blue for controls, red for AsymAD cases, and green for AD cases. Amyloid immunoassay measures of 1,700 (maximum, saturated value in the assay) were not considered for correlation.

Figure 7. Receiver-operating characteristic (ROC) curve analysis of peptide diagnostic potential. ROC curves for each of three pairs of diagnosed case groups were generated to determine the top-ranked diagnostic biomarker peptides among the 58-peptide panel plus 4 APOE specific peptides. (**A**) A total of 263 AD (N=130) and control (N=133) CSF case samples were classified according to the logistic fit for each peptide's log_2(ratio) measurements across these samples, and the top 5 ranked by AUC are shown. (**B**) Top five performing peptides for discerning AsymAD (N=127) from control (N=133) case diagnosis groups are provided with AUCs, nominating these peptides as potential markers of pre-symptomatic disease, and as

cognates for AT+ biomarker positivity. (**C**) Symptomatic AD (N=130) and AsymAD (N=127) discerning peptides were ranked by AUC and the top five ROC curves are shown and nominated as cognate CSF measures for compromised patient cognition.

Supplemental Data

Supplemental Figure 1. Coefficients of variation (CV) plotted for 58 biomarker peptides in AT- and AT+ QC pools. The QC pools were measured (N=30) during the analysis of clinical samples. The CV (%) for 58 biomarker peptides measured in AT- (black, N=15) and AT+ (gray, N=15) was plotted to illustrate all biomarker peptides had a CV<20% in at least one QC pool. CV=20% is shown with a solid green line.

Supplemental Figure 2. Monitoring background peptide levels in CSF. Three proteins were monitored for levels of potential blood contamination in each of the CSF samples. The peptide ratio for hemoglobin subunit alpha (**A**), hemoglobin subunit beta (**B**), and albumin (**C** and **D**) peptides are plotted for each of the CSF samples (N=423) in acquisition order.

Supplemental Figure 3. Differentially abundant peptides representing changed proteins in AT- vs AT+ QC CSF pools. The differentially abundant proteins in the QC pools were used to check the accuracy of the fold change consistent with our other studies [18]. We found 21 upregulated and 10 downregulated peptides. This result validated the direction of change of six proteins nominally significantly downregulated in previously published discovery proteomics (PON1, APOC1, NPTX2, VGF, NPTXR, and SCG2), and of sixteen proteins previously reported as upregulated (YWHAZ, GDA, CHI3L1, PKM, CALM2, SMOC1, YWHAB, MDH1, ALDOA, ENO1, GOT1, PPIA, DDAH1, PEBP1, PARK7, and SPP1) [18, 23].

Supplemental Table 1. Coefficient of variation (CV) values for 58 biomarker peptides and APOE allele specific peptides in AT- and AT+ QC pools.

Supplemental Table 2. ANOVA of differential abundance analysis for 58 biomarker peptides across Control, AsymAD and AD sample pairwise group comparisons.

Supplemental Table 3. Pearson correlations (rho), Student p values of correlation significance, and numbers of paired observations for correlation of biomarker peptide abundances to immunoassay measures of Aβ(1-42), total Tau, phospho-T181 Tau, and the ratio of total Tau/ Aβ.

Supplemental Table 4. ROC curve statistics including AUC, p, 95% DeLong confidence interval, accuracy, specificity, and sensitivity for dichotomous diagnosis case sample groups.

References

1. *2019 Alzheimer's Disease Facts and Figures Report*; Available at: https://www.alz.org/media/Documents/alzheimers-facts-and-figures-2019-r.pdf 2019.
2. *World Alzheimer Report 2015: the Global Impact of Dementia: An Analysis of Prevalence, Incidence, Cost and Trends*; Alzheimer's Disease International (ADI): ADI website. https://www.alz.co.uk/research/WorldAlzheimerReport2015.pdf. Published 2015. Accessed March 20, 2018., 2015.
3. Scheltens, P.; De Strooper, B.; Kivipelto, M.; Holstege, H.; Chételat, G.; Teunissen, C. E.; Cummings, J.; van der Flier, W. M., Alzheimer's disease. *The Lancet* **2021,** *397* (10284), 1577-1590.
4. Duyckaerts, C.; Delatour, B.; Potier, M.-C., Classification and basic pathology of Alzheimer disease. *Acta neuropathologica* **2009,** *118* (1), 5-36.
5. Jack Jr, C. R.; Bennett, D. A.; Blennow, K.; Carrillo, M. C.; Dunn, B.; Haeberlein, S. B.; Holtzman, D. M.; Jagust, W.; Jessen, F.; Karlawish, J., NIA-AA research framework: toward a biological definition of Alzheimer's disease. *Alzheimer's & Dementia* **2018,** *14* (4), 535-562.
6. Mattsson-Carlgren, N.; Grinberg, L. T.; Boxer, A.; Ossenkoppele, R.; Jonsson, M.; Seeley, W.; Ehrenberg, A.; Spina, S.; Janelidze, S.; Rojas-Martinex, J., Cerebrospinal fluid biomarkers in autopsy-confirmed Alzheimer disease and frontotemporal lobar degeneration. *Neurology* **2022,** *98* (11), e1137-e1150.
7. Zetterberg, H.; Blennow, K., Moving fluid biomarkers for Alzheimer's disease from research tools to routine clinical diagnostics. *Molecular neurodegeneration* **2021,** *16* (1), 1-7.
8. Long, J. M.; Holtzman, D. M., Alzheimer disease: an update on pathobiology and treatment strategies. *Cell* **2019,** *179* (2), 312-339.
9. Rayaprolu, S.; Higginbotham, L.; Bagchi, P.; Watson, C. M.; Zhang, T.; Levey, A. I.; Rangaraju, S.; Seyfried, N. T., Systems-based proteomics to resolve the biology of Alzheimer's disease beyond amyloid and tau. *Neuropsychopharmacology* **2021,** *46* (1), 98-115.
10. Sperling, R. A.; Aisen, P. S.; Beckett, L. A.; Bennett, D. A.; Craft, S.; Fagan, A. M.; Iwatsubo, T.; Jack Jr, C. R.; Kaye, J.; Montine, T. J., Toward defining the preclinical stages of Alzheimer's disease: Recommendations from the National Institute on Aging-Alzheimer's Association workgroups on diagnostic guidelines for Alzheimer's disease. *Alzheimer's & dementia* **2011,** *7* (3), 280-292.
11. Dubois, B.; Hampel, H.; Feldman, H. H.; Scheltens, P.; Aisen, P.; Andrieu, S.; Bakardjian, H.; Benali, H.; Bertram, L.; Blennow, K., Preclinical Alzheimer's disease: definition, natural history, and diagnostic criteria. *Alzheimer's & Dementia* **2016,** *12* (3), 292-323.
12. Hasin, Y.; Seldin, M.; Lusis, A., Multi-omics approaches to disease. *Genome biology* **2017,** *18* (1), 1-15.
13. Seyfried, N. T.; Dammer, E. B.; Swarup, V.; Nandakumar, D.; Duong, D. M.; Yin, L.; Deng, Q.; Nguyen, T.; Hales, C. M.; Wingo, T.; Glass, J.; Gearing, M.; Thambisetty, M.; Troncoso, J. C.; Geschwind, D. H.; Lah, J. J.; Levey, A. I., A Multi-network Approach Identifies Protein-Specific Co-expression in Asymptomatic and Symptomatic Alzheimer's Disease. *Cell Syst* **2017,** *4* (1), 60-72 e4.
14. Johnson, E. C. B.; Dammer, E. B.; Duong, D. M.; Yin, L.; Thambisetty, M.; Troncoso, J. C.; Lah, J. J.; Levey, A. I.; Seyfried, N. T., Deep proteomic network analysis of Alzheimer's disease brain reveals alterations in RNA binding proteins and RNA splicing associated with disease. *Mol Neurodegener* **2018,** *13* (1), 52.
15. Johnson, E. C. B.; Dammer, E. B.; Duong, D. M.; Ping, L.; Zhou, M.; Yin, L.; Higginbotham, L. A.; Guajardo, A.; White, B.; Troncoso, J. C.; Thambisetty, M.; Montine, T. J.; Lee, E. B.; Trojanowski, J. Q.; Beach, T. G.; Reiman, E. M.; Haroutunian, V.; Wang, M.; Schadt, E.; Zhang, B.; Dickson, D. W.; Ertekin-Taner, N.; Golde, T. E.; Petyuk, V. A.; De Jager, P. L.; Bennett, D. A.; Wingo, T. S.; Rangaraju, S.; Hajjar, I.; Shulman, J. M.; Lah, J. J.; Levey, A. I.; Seyfried, N. T., A Consensus Proteomic Analysis of

Alzheimer's Disease Brain and Cerebrospinal Fluid Reveals Early Changes in Energy Metabolism Associated with Microglia and Astrocyte Activation. *bioRxiv* **2019**, 802959.

16. Johnson, E. C.; Dammer, E. B.; Duong, D. M.; Ping, L.; Zhou, M.; Yin, L.; Higginbotham, L. A.; Guajardo, A.; White, B.; Troncoso, J. C., Large-scale proteomic analysis of Alzheimer's disease brain and cerebrospinal fluid reveals early changes in energy metabolism associated with microglia and astrocyte activation. *Nature medicine* **2020,** *26* (5), 769-780.

17. Blennow, K.; Zetterberg, H., Biomarkers for Alzheimer's disease: current status and prospects for the future. *Journal of internal medicine* **2018,** *284* (6), 643-663.

18. Higginbotham, L.; Ping, L.; Dammer, E. B.; Duong, D. M.; Zhou, M.; Gearing, M.; Hurst, C.; Glass, J. D.; Factor, S. A.; Johnson, E. C., Integrated proteomics reveals brain-based cerebrospinal fluid biomarkers in asymptomatic and symptomatic Alzheimer's disease. *Science advances* **2020,** *6* (43), eaaz9360.

19. Picotti, P.; Aebersold, R., Selected reaction monitoring–based proteomics: workflows, potential, pitfalls and future directions. *Nature methods* **2012,** *9* (6), 555-566.

20. Bittner, T.; Zetterberg, H.; Teunissen, C. E.; Ostlund, R. E., Jr.; Militello, M.; Andreasson, U.; Hubeek, I.; Gibson, D.; Chu, D. C.; Eichenlaub, U.; Heiss, P.; Kobold, U.; Leinenbach, A.; Madin, K.; Manuilova, E.; Rabe, C.; Blennow, K., Technical performance of a novel, fully automated electrochemiluminescence immunoassay for the quantitation of beta-amyloid (1-42) in human cerebrospinal fluid. *Alzheimers Dement* **2016,** *12* (5), 517-26.

21. Hansson, O.; Seibyl, J.; Stomrud, E.; Zetterberg, H.; Trojanowski, J. Q.; Bittner, T.; Lifke, V.; Corradini, V.; Eichenlaub, U.; Batrla, R.; Buck, K.; Zink, K.; Rabe, C.; Blennow, K.; Shaw, L. M.; Swedish Bio, F. s. g.; Alzheimer's Disease Neuroimaging, I., CSF biomarkers of Alzheimer's disease concord with amyloid-beta PET and predict clinical progression: A study of fully automated immunoassays in BioFINDER and ADNI cohorts. *Alzheimers Dement* **2018,** *14* (11), 1470-1481.

22. Schindler, S. E.; Gray, J. D.; Gordon, B. A.; Xiong, C.; Batrla-Utermann, R.; Quan, M.; Wahl, S.; Benzinger, T. L. S.; Holtzman, D. M.; Morris, J. C.; Fagan, A. M., Cerebrospinal fluid biomarkers measured by Elecsys assays compared to amyloid imaging. *Alzheimers Dement* **2018**.

23. Zhou, M.; Haque, R. U.; Dammer, E. B.; Duong, D. M.; Ping, L.; Johnson, E. C.; Lah, J. J.; Levey, A. I.; Seyfried, N. T., Targeted mass spectrometry to quantify brain-derived cerebrospinal fluid biomarkers in Alzheimer's disease. *Clinical Proteomics* **2020,** *17*, 1-14.

24. MacLean, B.; Tomazela, D. M.; Shulman, N.; Chambers, M.; Finney, G. L.; Frewen, B.; Kern, R.; Tabb, D. L.; Liebler, D. C.; MacCoss, M. J., Skyline: an open source document editor for creating and analyzing targeted proteomics experiments. *Bioinformatics* **2010,** *26* (7), 966-968.

25. Pino, L. K.; Searle, B. C.; Bollinger, J. G.; Nunn, B.; MacLean, B.; MacCoss, M. J., The Skyline ecosystem: Informatics for quantitative mass spectrometry proteomics. *Mass spectrometry reviews* **2020,** *39* (3), 229-244.

26. MacLean, B.; Tomazela, D. M.; Abbatiello, S. E.; Zhang, S.; Whiteaker, J. R.; Paulovich, A. G.; Carr, S. A.; MacCoss, M. J., Effect of collision energy optimization on the measurement of peptides by selected reaction monitoring (SRM) mass spectrometry. *Analytical chemistry* **2010,** *82* (24), 10116-10124.

27. Kulak, N. A.; Pichler, G.; Paron, I.; Nagaraj, N.; Mann, M., Minimal, encapsulated proteomic-sample processing applied to copy-number estimation in eukaryotic cells. *Nature methods* **2014,** *11* (3), 319-324.

28. Simon, R.; Girod, M.; Fonbonne, C.; Salvador, A.; Clement, Y.; Lanteri, P.; Amouyel, P.; Lambert, J. C.; Lemoine, J., Total ApoE and ApoE4 isoform assays in an Alzheimer's disease case-control study by targeted mass spectrometry (n= 669): a pilot assay for methionine-containing proteotypic peptides. *Molecular & Cellular Proteomics* **2012,** *11* (11), 1389-1403.

29. Rezeli, M.; Zetterberg, H.; Blennow, K.; Brinkmalm, A.; Laurell, T.; Hansson, O.; Marko-Varga, G., Quantification of total apolipoprotein E and its specific isoforms in cerebrospinal fluid and blood in Alzheimer's disease and other neurodegenerative diseases. *EuPA Open Proteomics* **2015,** *8*, 137-143.
30. Geyer, P. E.; Voytik, E.; Treit, P. V.; Doll, S.; Kleinhempel, A.; Niu, L.; Müller, J. B.; Buchholtz, M. L.; Bader, J. M.; Teupser, D., Plasma Proteome Profiling to detect and avoid sample-related biases in biomarker studies. *EMBO molecular medicine* **2019,** *11* (11), e10427.
31. Beri, J.; Rosenblatt, M. M.; Strauss, E.; Urh, M.; Bereman, M. S., Reagent for evaluating liquid chromatography–tandem mass spectrometry (LC-MS/MS) performance in bottom-up proteomic experiments. *Analytical chemistry* **2015,** *87* (23), 11635-11640.
32. Hatters, D. M.; Peters-Libeu, C. A.; Weisgraber, K. H., Apolipoprotein E structure: insights into function. *Trends in biochemical sciences* **2006,** *31* (8), 445-454.
33. Saunders, A. M.; Strittmatter, W. J.; Schmechel, D.; George-Hyslop, P. S.; Pericak-Vance, M. A.; Joo, S.; Rosi, B.; Gusella, J.; Crapper-MacLachlan, D.; Alberts, M., Association of apolipoprotein E allele ϵ4 with late-onset familial and sporadic Alzheimer's disease. *Neurology* **1993,** *43* (8), 1467-1467.
34. Farrer, L. A.; Cupples, L. A.; Haines, J. L.; Hyman, B.; Kukull, W. A.; Mayeux, R.; Myers, R. H.; Pericak-Vance, M. A.; Risch, N.; van Duijn, C. M., Effects of age, sex, and ethnicity on the association between apolipoprotein E genotype and Alzheimer disease. A meta-analysis. APOE and Alzheimer Disease Meta Analysis Consortium. *JAMA* **1997,** *278* (16), 1349-56.
35. Heffernan, A. L.; Chidgey, C.; Peng, P.; Masters, C. L.; Roberts, B. R., The neurobiology and age-related prevalence of the ε4 allele of apolipoprotein E in Alzheimer's disease cohorts. *Journal of Molecular Neuroscience* **2016,** *60* (3), 316-324.
36. Minta, K.; Brinkmalm, G.; Janelidze, S.; Sjödin, S.; Portelius, E.; Stomrud, E.; Zetterberg, H.; Blennow, K.; Hansson, O.; Andreasson, U., Quantification of total apolipoprotein E and its isoforms in cerebrospinal fluid from patients with neurodegenerative diseases. *Alzheimer's research & therapy* **2020,** *12* (1), 1-11.
37. Bussy, A.; Snider, B. J.; Coble, D.; Xiong, C.; Fagan, A. M.; Cruchaga, C.; Benzinger, T. L.; Gordon, B. A.; Hassenstab, J.; Bateman, R. J., Effect of apolipoprotein E4 on clinical, neuroimaging, and biomarker measures in noncarrier participants in the Dominantly Inherited Alzheimer Network. *Neurobiology of aging* **2019,** *75*, 42-50.
38. El-Lebedy, D.; Raslan, H. M.; Mohammed, A. M., Apolipoprotein E gene polymorphism and risk of type 2 diabetes and cardiovascular disease. *Cardiovascular diabetology* **2016,** *15* (1), 1-11.
39. Morris, J. C.; Roe, C. M.; Xiong, C.; Fagan, A. M.; Goate, A. M.; Holtzman, D. M.; Mintun, M. A., APOE predicts amyloid-beta but not tau Alzheimer pathology in cognitively normal aging. *Ann Neurol* **2010,** *67* (1), 122-31.
40. Grimmer, T.; Tholen, S.; Yousefi, B. H.; Alexopoulos, P.; Förschler, A.; Förstl, H.; Henriksen, G.; Klunk, W. E.; Mathis, C. A.; Perneczky, R., Progression of cerebral amyloid load is associated with the apolipoprotein E ε4 genotype in Alzheimer's disease. *Biological psychiatry* **2010,** *68* (10), 879-884.
41. Knopman, D. S.; Haeberlein, S. B.; Carrillo, M. C.; Hendrix, J. A.; Kerchner, G.; Margolin, R.; Maruff, P.; Miller, D. S.; Tong, G.; Tome, M. B., The National Institute on Aging and the Alzheimer's Association research framework for Alzheimer's disease: perspectives from the research roundtable. *Alzheimer's & Dementia* **2018,** *14* (4), 563-575.
42. Wingo, A. P.; Dammer, E. B.; Breen, M. S.; Logsdon, B. A.; Duong, D. M.; Troncosco, J. C.; Thambisetty, M.; Beach, T. G.; Serrano, G. E.; Reiman, E. M., Large-scale proteomic analysis of human brain identifies proteins associated with cognitive trajectory in advanced age. *Nature communications* **2019,** *10* (1), 1-14.
43. Dammer, E. B.; Ping, L.; Duong, D. M.; Modeste, E. S.; Seyfried, N. T.; Lah, J. J.; Levey, A. I.; Johnson, E. C., Multi-Platform Proteomic Analysis of Alzheimer's Disease Cerebrospinal Fluid and Plasma Reveals Network Biomarkers Associated with Proteostasis and the Matrisome. *bioRxiv* **2022**.

44. Bertens, D.; Knol, D. L.; Scheltens, P.; Visser, P. J., Temporal evolution of biomarkers and cognitive markers in the asymptomatic, MCI, and dementia stage of Alzheimer's disease. *Alzheimer's & Dementia* **2015,** *11* (5), 511-522.
45. Shokouhi, S.; McKay, J. W.; Baker, S. L.; Kang, H.; Brill, A. B.; Gwirtsman, H. E.; Riddle, W. R.; Claassen, D. O.; Rogers, B. P.; for the Alzheimer's Disease Neuroimaging, I., Reference tissue normalization in longitudinal 18F-florbetapir positron emission tomography of late mild cognitive impairment. *Alzheimer's Research & Therapy* **2016,** *8* (1), 2.
46. Sathe, G.; Na, C. H.; Renuse, S.; Madugundu, A. K.; Albert, M.; Moghekar, A.; Pandey, A., Quantitative proteomic profiling of cerebrospinal fluid to identify candidate biomarkers for Alzheimer's disease. *PROTEOMICS–Clinical Applications* **2019,** *13* (4), 1800105.
47. Bader, J. M.; Geyer, P. E.; Müller, J. B.; Strauss, M. T.; Koch, M.; Leypoldt, F.; Koertvelyessy, P.; Bittner, D.; Schipke, C. G.; Incesoy, E. I., Proteome profiling in cerebrospinal fluid reveals novel biomarkers of Alzheimer's disease. *Molecular systems biology* **2020,** *16* (6), e9356.
48. Libiger, O.; Shaw, L. M.; Watson, M. H.; Nairn, A. C.; Umana, K. L.; Biarnes, M. C.; Canet-Avilés, R. M.; Jack Jr, C. R.; Breton, Y. A.; Cortes, L., Longitudinal CSF proteomics identifies NPTX2 as a prognostic biomarker of Alzheimer's disease. *Alzheimer's & Dementia* **2021,** *17* (12), 1976-1987.

Table 1. Cohort Characteristics

Sample Group	CT	AsymAD	AD
Sample Size	N=133	N=127	N=130
Characteristics			
Sex	99 F, 34 M	94 F, 33 M	97 F, 33 M
Age [a]	66 ± 6	66 ± 6	66 ± 6
MoCA [b]	26.8 ± 2.0	26.4 ± 2.6	17.4 ± 5.5
$A\beta_{42}$ [b]	1394.0 ± 280.7	752.0 ± 238.2	587.0 ± 236.8
tTau [b]	165.8 ± 35.0	260.8 ± 97.2	375.7 ± 139.6
pTau [b]	14.7 ± 3.2	25.2 ± 11.1	38.5 ± 15.5

[a] Age in years. Values given as average ± standard deviation

[b] MoCA, $A\beta_{42}$, tTau, and pTau in pg/mL. Values given in average ± standard deviation

Abbreviations: CT, Control; AD, Alzheimer's disease; MoCA, Montreal Cognitive Assessment

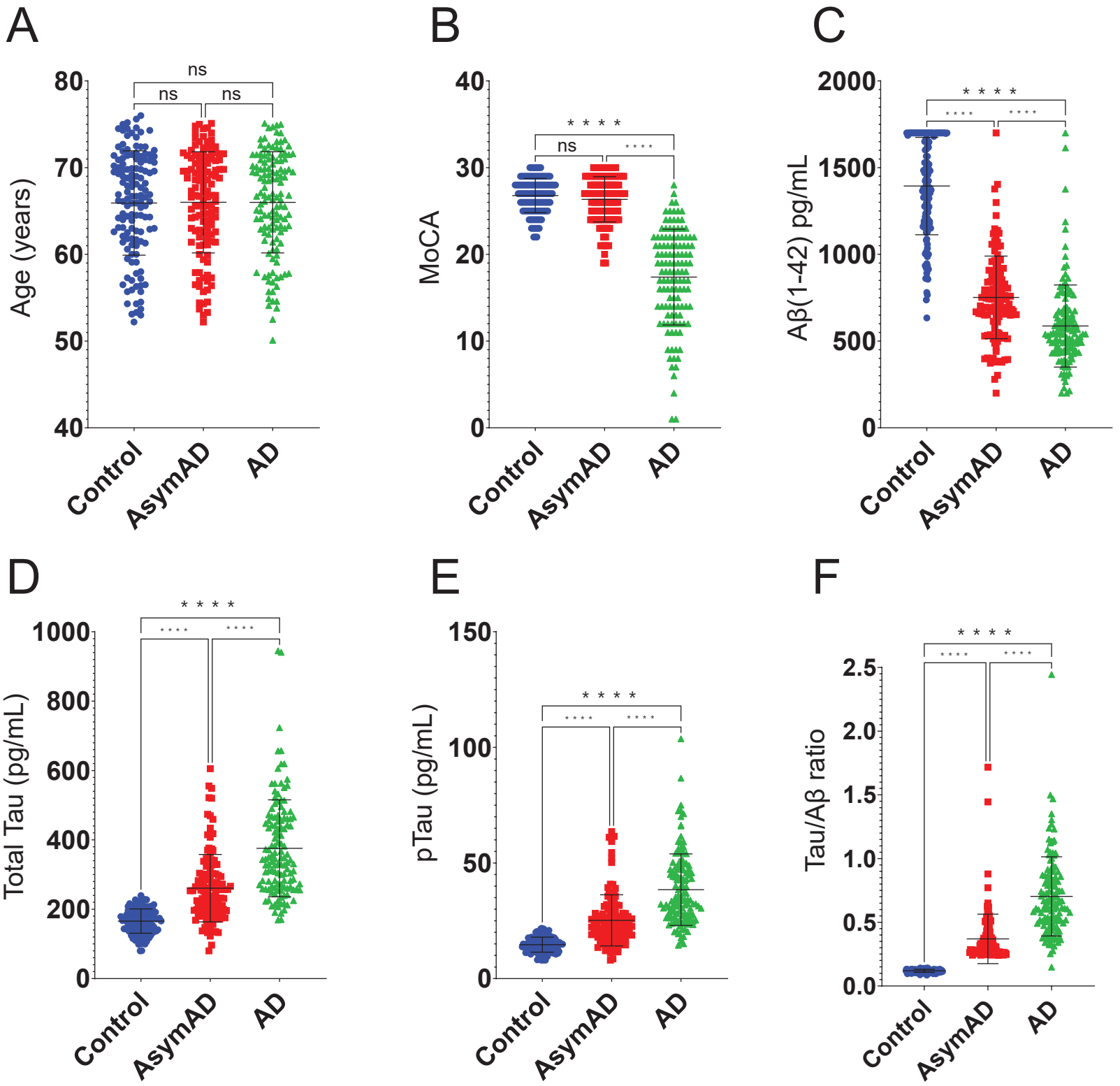
A
B
C
D
E
F
Age (years)
MoCA
Aβ(1-42) pg/mL
Total Tau (pg/mL)
pTau (pg/mL)
Tau/Aβ ratio
Control
AsymAD
AD
ns
* * * *

Figure 2

A

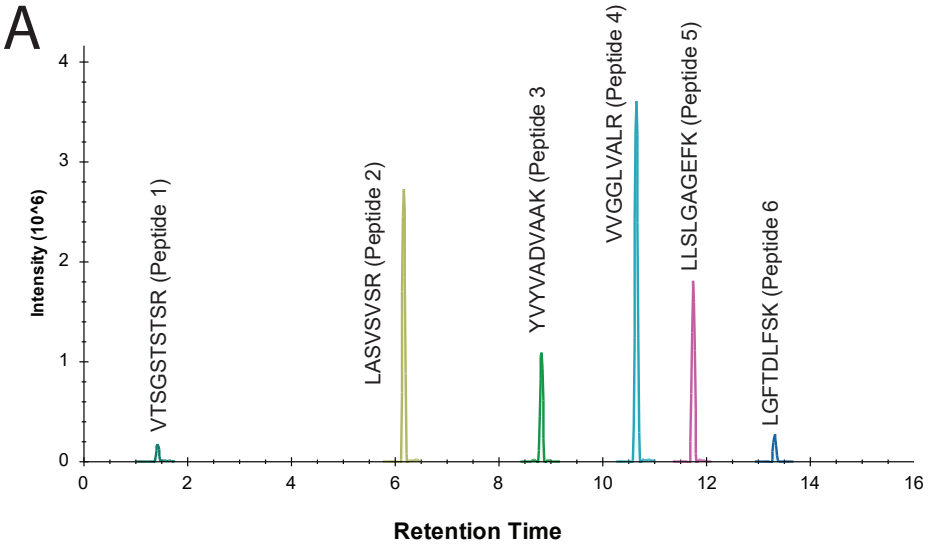

B

Promega Peptide Sequence	Average Retention Time (min)	1 pmole (1x)	100 fmole (0.1x)	10 fmole (0.01x)	1 fmole (0.001x)	100 amole (0.0001x)
VTSGSTSTSR	1.42	17%	17%	18%	34%	ND
LASVSVSR	6.17	7%	8%	8%	17%	ND
YVYVADVAAK	8.83	11%	11%	13%	32%	ND
VVGGLVALR	10.65	8%	8%	9%	20%	ND
LLSLGAGEFK	11.75	9%	9%	10%	20%	ND
LGFTDLFSK	13.33	21%	21%	30%	ND	ND

C

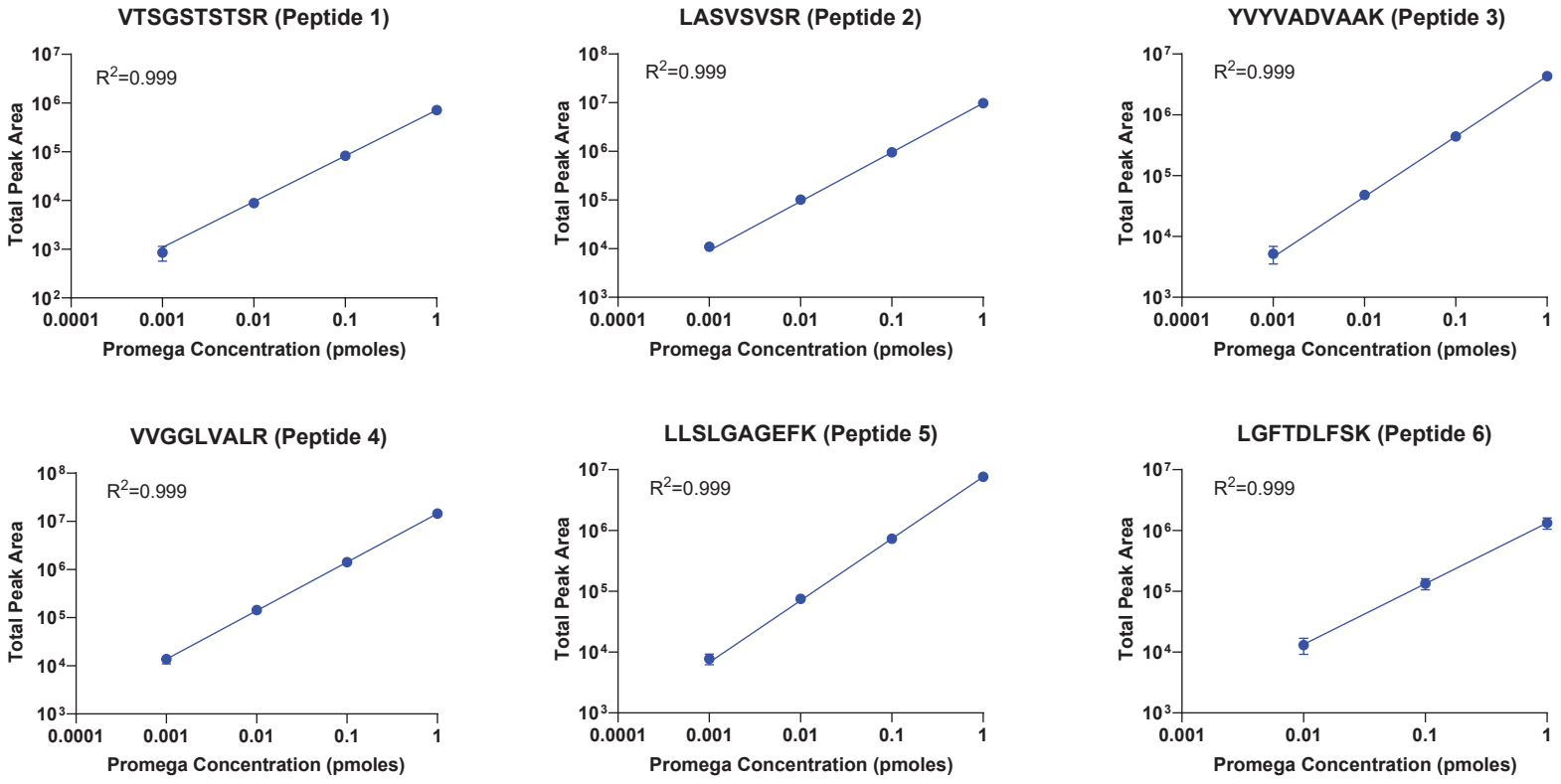

Figure 3

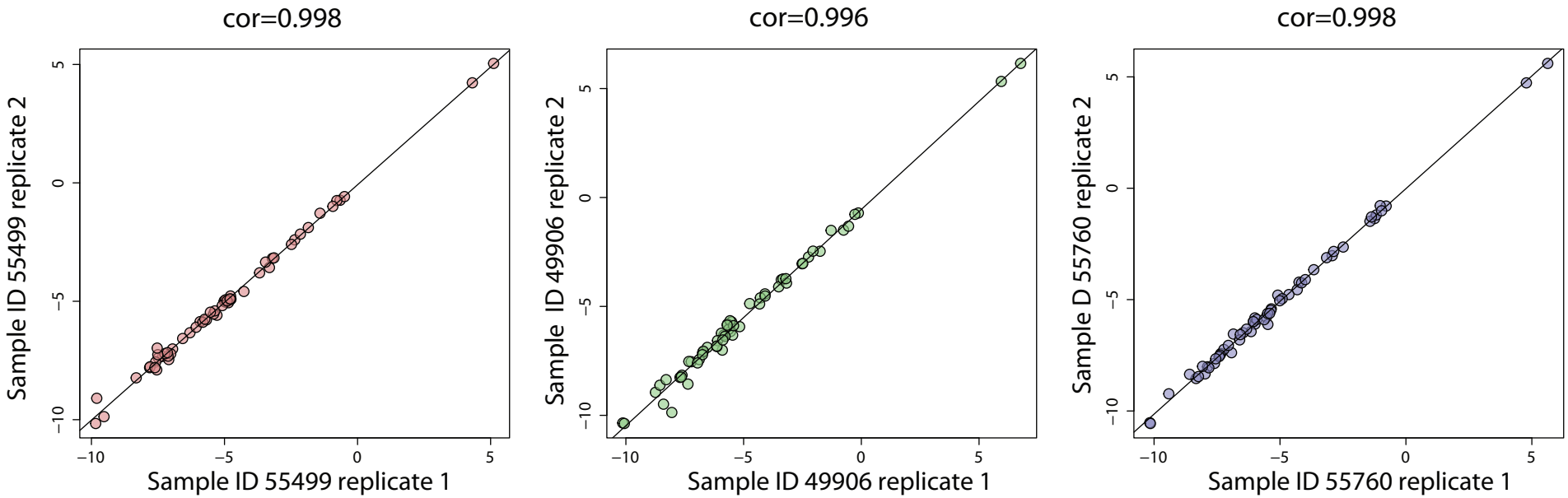
cor=0.998
Sample ID 55499 replicate 2
Sample ID 55499 replicate 1
cor=0.996
Sample ID 49906 replicate 2
Sample ID 49906 replicate 1
cor=0.998
Sample D 55760 replicate 2
Sample ID 55760 replicate 1
−10
−5
0
5

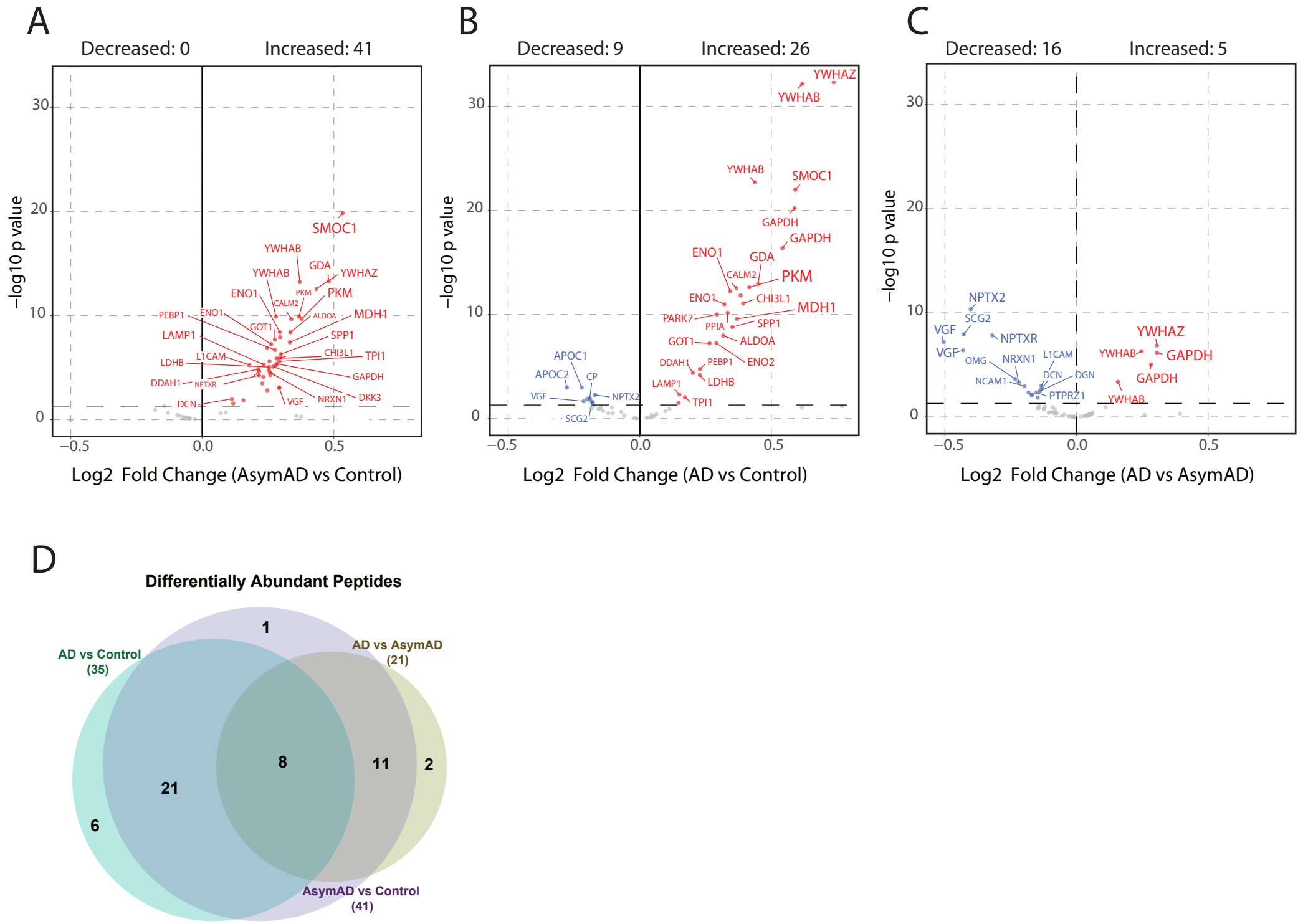
A
Decreased: 0
Increased: 41
−log10 p value
Log2 Fold Change (AsymAD vs Control)
SMOC1
YWHAB
GDA
YWHAZ
ENO1
PKM
CALM2
PEBP1
ALDOA
MDH1
GOT1
LAMP1
SPP1
L1CAM
CHI3L1
TPI1
LDHB
GAPDH
DDAH1
NPTXR
DKK3
DCN
VGF
NRXN1
B
Decreased: 9
Increased: 26
Log2 Fold Change (AD vs Control)
YWHAZ
YWHAB
SMOC1
GAPDH
GAPDH
ENO1
GDA
CALM2
PKM
ENO1
CHI3L1
MDH1
PARK7
PPIA
SPP1
GOT1
ALDOA
APOC1
DDAH1
PEBP1
ENO2
APOC2
CP
LDHB
LAMP1
VGF
NPTX2
TPI1
SCG2
C
Decreased: 16
Increased: 5
Log2 Fold Change (AD vs AsymAD)
NPTX2
SCG2
VGF
NPTXR
YWHAZ
VGF
YWHAB
GAPDH
OMG
NRXN1
L1CAM
NCAM1
DCN
OGN
GAPDH
PTPRZ1
YWHAB
D
Differentially Abundant Peptides
AD vs Control
(35)
AD vs AsymAD
(21)
AsymAD vs Control
(41)
1
8
11
2
21
6

Figure 5

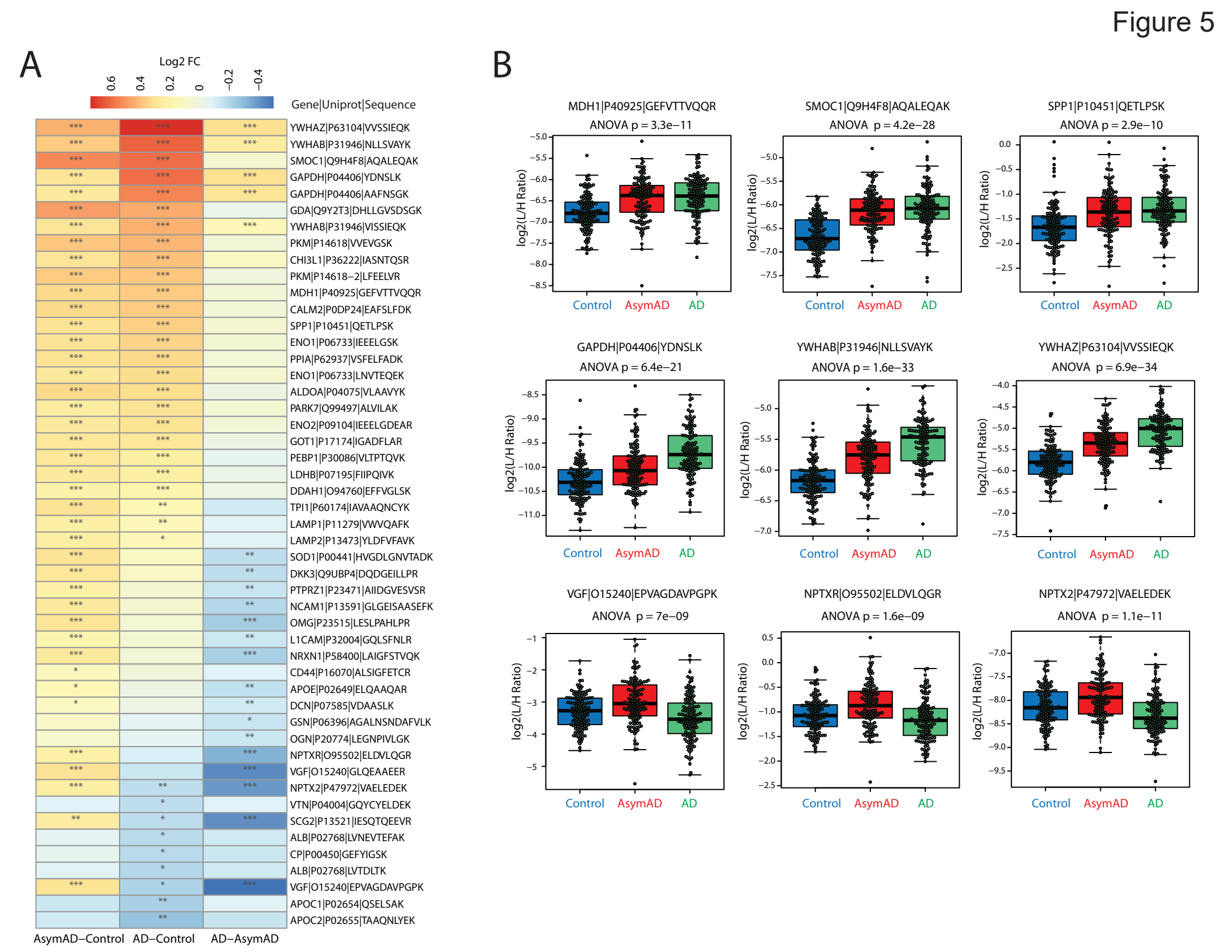
A
Log2 FC
0.6
0.4
0.2
0
−0.2
−0.4
Gene|Uniprot|Sequence
YWHAZ|P63104|VVSSIEQK
YWHAB|P31946|NLLSVAYK
SMOC1|Q9H4F8|AQALEQAK
GAPDH|P04406|YDNSLK
GAPDH|P04406|AAFNSGK
GDA|Q9Y2T3|DHLLGVSDSGK
YWHAB|P31946|VISSIEQK
PKM|P14618|VVEVGSK
CHI3L1|P36222|IASNTQSR
PKM|P14618−2|LFEELVR
MDH1|P40925|GEFVTTVQQR
CALM2|P0DP24|EAFSLFDK
SPP1|P10451|QETLPSK
ENO1|P06733|IEEELGSK
PPIA|P62937|VSFELFADK
ENO1|P06733|LNVTEQEK
ALDOA|P04075|VLAAVYK
PARK7|Q99497|ALVILAK
ENO2|P09104|IEEELGDEAR
GOT1|P17174|IGADFLAR
PEBP1|P30086|VLTPTQVK
LDHB|P07195|FIIPQIVK
DDAH1|O94760|EFFVGLSK
TPI1|P60174|IAVAAQNCYK
LAMP1|P11279|VWVQAFK
LAMP2|P13473|YLDFVFAVK
SOD1|P00441|HVGDLGNVTADK
DKK3|Q9UBP4|DQDGEILLPR
PTPRZ1|P23471|AIIDGVESVSR
NCAM1|P13591|GLGEISAASEFK
OMG|P23515|LESLPAHLPR
L1CAM|P32004|GQLSFNLR
NRXN1|P58400|LAIGFSTVQK
CD44|P16070|ALSIGFETCR
APOE|P02649|ELQAAQAR
DCN|P07585|VDAASLK
GSN|P06396|AGALNSNDAFVLK
OGN|P20774|LEGNPIVLGK
NPTXR|O95502|ELDVLQGR
VGF|O15240|GLQEAAEER
NPTX2|P47972|VAELEDEK
VTN|P04004|GQYCYELDEK
SCG2|P13521|IESQTQEEVR
ALB|P02768|LVNEVTEFAK
CP|P00450|GEFYIGSK
ALB|P02768|LVTDLTK
VGF|O15240|EPVAGDAVPGPK
APOC1|P02654|QSELSAK
APOC2|P02655|TAAQNLYEK
AsymAD−Control
AD−Control
AD−AsymAD
B
MDH1|P40925|GEFVTTVQQR
ANOVA p = 3.3e−11
SMOC1|Q9H4F8|AQALEQAK
ANOVA p = 4.2e−28
SPP1|P10451|QETLPSK
ANOVA p = 2.9e−10
GAPDH|P04406|YDNSLK
ANOVA p = 6.4e−21
YWHAB|P31946|NLLSVAYK
ANOVA p = 1.6e−33
YWHAZ|P63104|VVSSIEQK
ANOVA p = 6.9e−34
VGF|O15240|EPVAGDAVPGPK
ANOVA p = 7e−09
NPTXR|O95502|ELDVLQGR
ANOVA p = 1.6e−09
NPTX2|P47972|VAELEDEK
ANOVA p = 1.1e−11
log2(L/H Ratio)
Control
AsymAD
AD

Figure 6

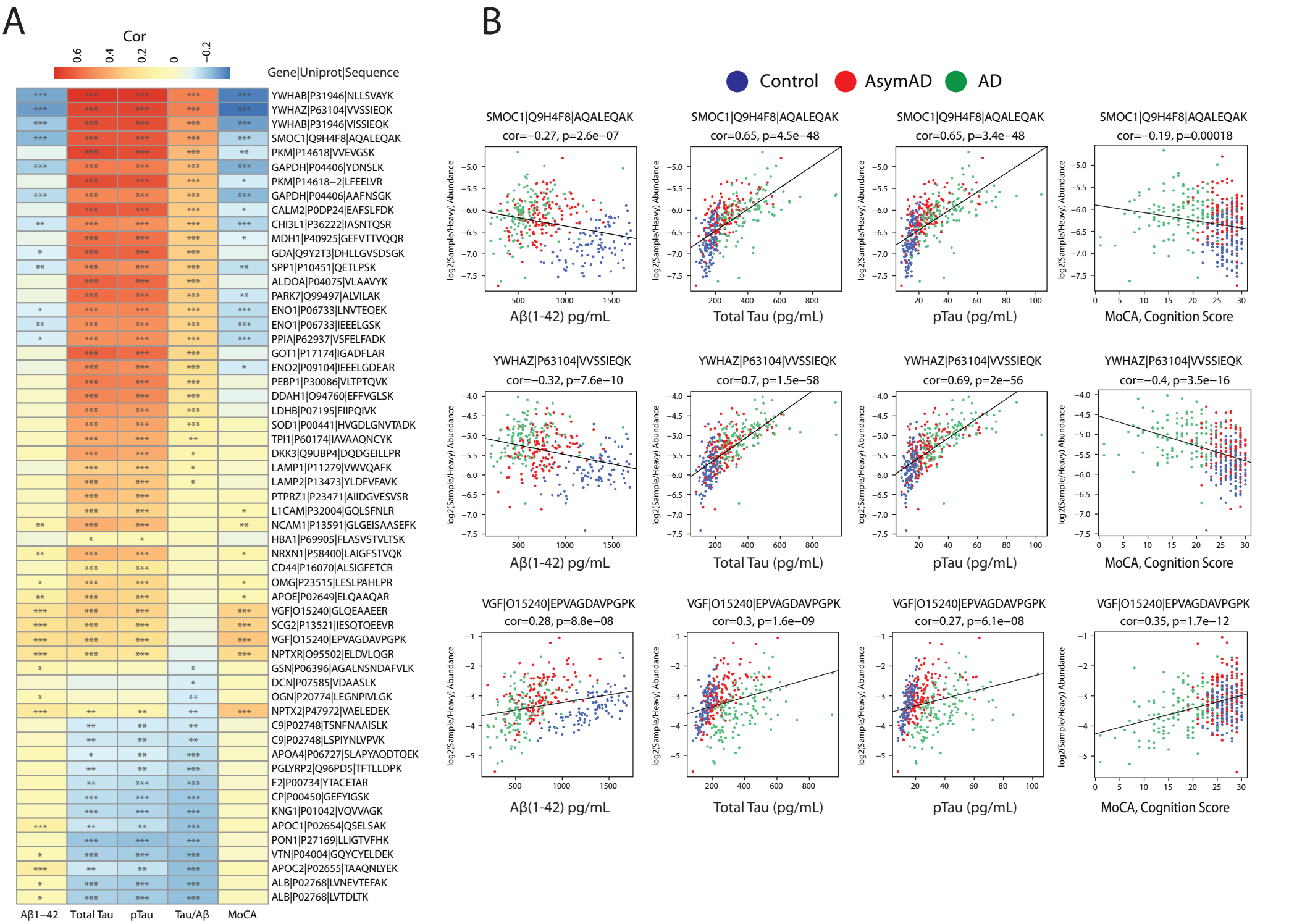
A
Cor
0.6
0.4
0.2
0
−0.2
Gene|Uniprot|Sequence
YWHAB|P31946|NLLSVAYK
YWHAZ|P63104|VVSSIEQK
YWHAB|P31946|VISSIEQK
SMOC1|Q9H4F8|AQALEQAK
PKM|P14618|VVEVGSK
GAPDH|P04406|YDNSLK
PKM|P14618−2|LFEELVR
GAPDH|P04406|AAFNSGK
CALM2|P0DP24|EAFSLFDK
CHI3L1|P36222|IASNTQSR
MDH1|P40925|GEFVTTVQQR
GDA|Q9Y2T3|DHLLGVSDSGK
SPP1|P10451|QETLPSK
ALDOA|P04075|VLAAVYK
PARK7|Q99497|ALVILAK
ENO1|P06733|LNVTEQEK
ENO1|P06733|IEEELGSK
PPIA|P62937|VSFELFADK
GOT1|P17174|IGADFLAR
ENO2|P09104|IEEELGDEAR
PEBP1|P30086|VLTPTQVK
DDAH1|O94760|EFFVGLSK
LDHB|P07195|FIIPQIVK
SOD1|P00441|HVGDLGNVTADK
TPI1|P60174|IAVAAQNCYK
DKK3|Q9UBP4|DQDGEILLPR
LAMP1|P11279|VWVQAFK
LAMP2|P13473|YLDFVFAVK
PTPRZ1|P23471|AIIDGVESVSR
L1CAM|P32004|GQLSFNLR
NCAM1|P13591|GLGEISAASEFK
HBA1|P69905|FLASVSTVLTSK
NRXN1|P58400|LAIGFSTVQK
CD44|P16070|ALSIGFETCR
OMG|P23515|LESLPAHLPR
APOE|P02649|ELQAAQAR
VGF|O15240|GLQEAAEER
SCG2|P13521|IESQTQEEVR
VGF|O15240|EPVAGDAVPGPK
NPTXR|O95502|ELDVLQGR
GSN|P06396|AGALNSNDAFVLK
DCN|P07585|VDAASLK
OGN|P20774|LEGNPIVLGK
NPTX2|P47972|VAELEDEK
C9|P02748|TSNFNAAISLK
C9|P02748|LSPIYNLVPVK
APOA4|P06727|SLAPYAQDTQEK
PGLYRP2|Q96PD5|TFTLLDPK
F2|P00734|YTACETAR
CP|P00450|GEFYIGSK
KNG1|P01042|VQVVAGK
APOC1|P02654|QSELSAK
PON1|P27169|LLIGTVFHK
VTN|P04004|GQYCYELDEK
APOC2|P02655|TAAQNLYEK
ALB|P02768|LVNEVTEFAK
ALB|P02768|LVTDLTK
Aβ1−42
Total Tau
pTau
Tau/Aβ
MoCA
B
Control
AsymAD
AD
SMOC1|Q9H4F8|AQALEQAK
cor=−0.27, p=2.6e−07
cor=0.65, p=4.5e−48
cor=0.65, p=3.4e−48
cor=−0.19, p=0.00018
YWHAZ|P63104|VVSSIEQK
cor=−0.32, p=7.6e−10
cor=0.7, p=1.5e−58
cor=0.69, p=2e−56
cor=−0.4, p=3.5e−16
VGF|O15240|EPVAGDAVPGPK
cor=0.28, p=8.8e−08
cor=0.3, p=1.6e−09
cor=0.27, p=6.1e−08
cor=0.35, p=1.7e−12
log2(Sample/Heavy) Abundance
Aβ(1-42) pg/mL
Total Tau (pg/mL)
pTau (pg/mL)
MoCA, Cognition Score

Figure 7

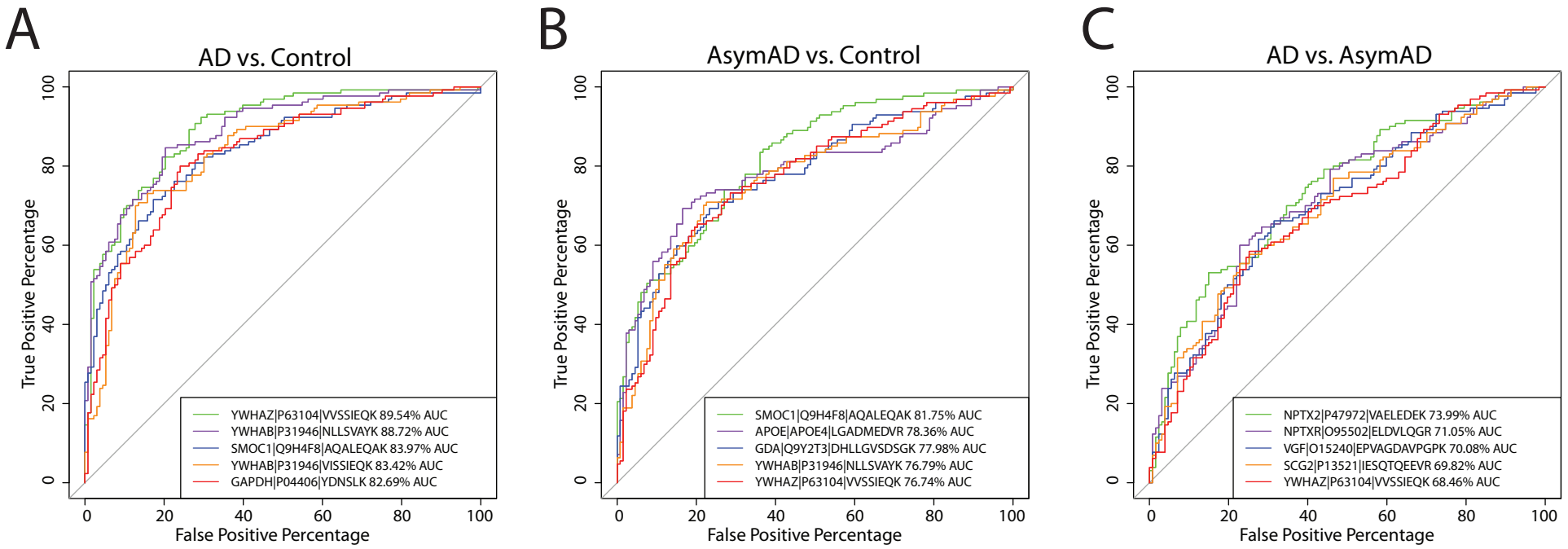
A
AD vs. Control
True Positive Percentage
False Positive Percentage
YWHAZ|P63104|VVSSIEQK 89.54% AUC
YWHAB|P31946|NLLSVAYK 88.72% AUC
SMOC1|Q9H4F8|AQALEQAK 83.97% AUC
YWHAB|P31946|VISSIEQK 83.42% AUC
GAPDH|P04406|YDNSLK 82.69% AUC
B
AsymAD vs. Control
True Positive Percentage
False Positive Percentage
SMOC1|Q9H4F8|AQALEQAK 81.75% AUC
APOE|APOE4|LGADMEDVR 78.36% AUC
GDA|Q9Y2T3|DHLLGVSDSGK 77.98% AUC
YWHAB|P31946|NLLSVAYK 76.79% AUC
YWHAZ|P63104|VVSSIEQK 76.74% AUC
C
AD vs. AsymAD
True Positive Percentage
False Positive Percentage
NPTX2|P47972|VAELEDEK 73.99% AUC
NPTXR|O95502|ELDVLQGR 71.05% AUC
VGF|O15240|EPVAGDAVPGPK 70.08% AUC
SCG2|P13521|IESQTQEEVR 69.82% AUC
YWHAZ|P63104|VVSSIEQK 68.46% AUC

Supplemental Figure 1

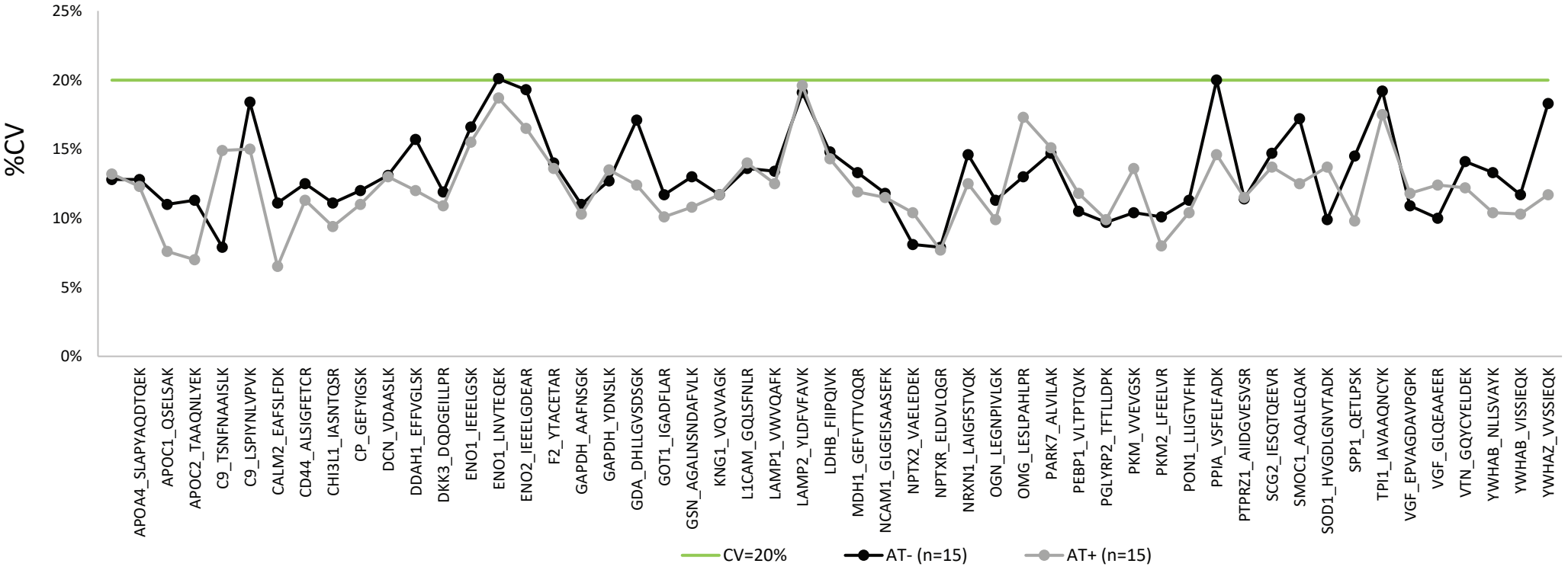

Supplemental Figure 2

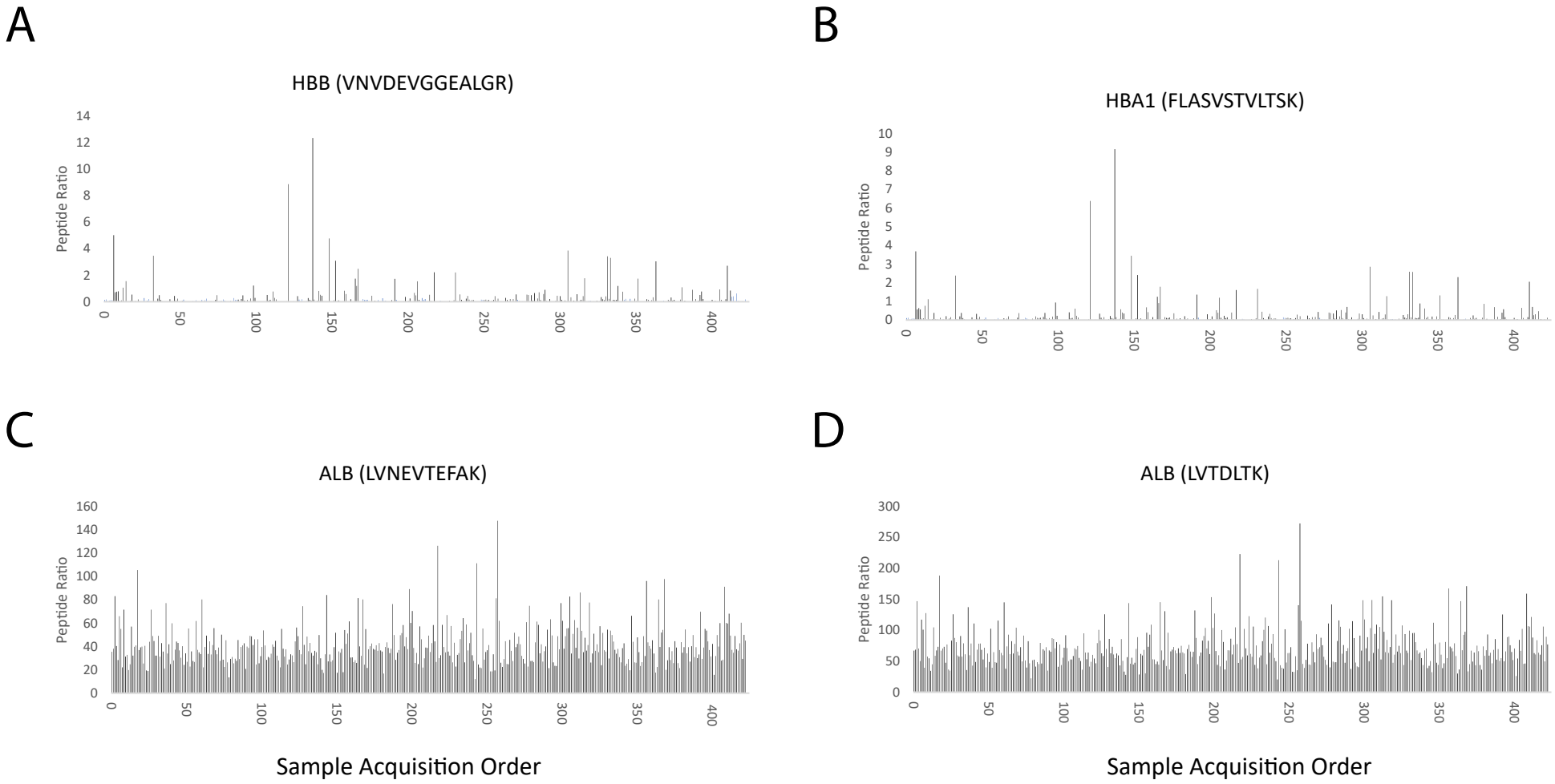

Supplemental Figure 3